



## Enhanced near-infrared response of nano- and microstructured silicon/organic hybrid photodetectors

Vedran Đerek, Eric Daniel Głowacki, Mykhailo Sytnyk, Wolfgang Heiss, Marijan Marciuš, Mira Ristić, Mile Ivanda, and Niyazi Serdar Sariciftci

Citation: *Applied Physics Letters* **107**, 083302 (2015); doi: 10.1063/1.4929841

View online: <http://dx.doi.org/10.1063/1.4929841>

View Table of Contents: <http://scitation.aip.org/content/aip/journal/apl/107/8?ver=pdfcov>

Published by the AIP Publishing

---

### Articles you may be interested in

[Improving the sensitivity of a near-infrared nanocomposite photodetector by enhancing trap induced hole injection](#)

Appl. Phys. Lett. **106**, 023301 (2015); 10.1063/1.4905930

[InGaN/silicon heterojunction based narrow band near-infrared detector](#)

J. Vac. Sci. Technol. B **33**, 011205 (2015); 10.1116/1.4904760

[n -type  \$\beta\$  - FeSi 2 /intrinsic- Si / p -type Si heterojunction photodiodes for near-infrared light detection at room temperature](#)

Appl. Phys. Lett. **95**, 162102 (2009); 10.1063/1.3250171

[Characterization of near-infrared n -type  \$\beta\$  -FeSi 2 / p -type Si heterojunction photodiodes at room temperature](#)

Appl. Phys. Lett. **94**, 222113 (2009); 10.1063/1.3151915

[Silicon membrane resonant-cavity-enhanced photodetector](#)

Appl. Phys. Lett. **87**, 061111 (2005); 10.1063/1.2009822

---

The image shows the cover of an Applied Physics Reviews journal. It features a blue and orange color scheme with a molecular structure background. The text 'AIP Applied Physics Reviews' is at the top left. The main title 'NEW Special Topic Sections' is in large white letters. Below it, 'NOW ONLINE' is in orange, followed by 'Lithium Niobate Properties and Applications: Reviews of Emerging Trends' in white. The AIP logo and 'Applied Physics Reviews' are at the bottom right.

## NEW Special Topic Sections

**NOW ONLINE**  
Lithium Niobate Properties and Applications:  
Reviews of Emerging Trends

**AIP** Applied Physics Reviews

# Enhanced near-infrared response of nano- and microstructured silicon/organic hybrid photodetectors

Vedran Derek,<sup>1</sup> Eric Daniel Głowacki,<sup>2,a)</sup> Mykhailo Sytnyk,<sup>3</sup> Wolfgang Heiss,<sup>3</sup> Marijan Marčiuš,<sup>1</sup> Mira Ristić,<sup>1</sup> Mile Ivanda,<sup>1,a)</sup> and Niyazi Serdar Sarıcıftci<sup>2</sup>

<sup>1</sup>Center of Excellence for Advanced Materials and Sensing Devices, Research Unit for New Functional Materials, Ruđer Bošković Institute, Bijenička c. 54, Zagreb 10000, Croatia

<sup>2</sup>Linz Institute for Organic Solar Cells (LIOS), Physical Chemistry, Johannes Kepler University, Altenbergerstraße 69, Linz 4040, Austria

<sup>3</sup>Materials for Electronics and Energy Technology (i-MEET), Friedrich-Alexander Universität Erlangen-Nürnberg, Martensstraße 7, 91058 Erlangen, Germany and Energie Campus Nürnberg (EnCN), Fürther Straße 250, Nürnberg 90429, Germany

(Received 19 June 2015; accepted 19 August 2015; published online 28 August 2015)

Heterojunctions between an organic semiconductor and silicon are an attractive route to extending the response of silicon photodiodes into the near infrared (NIR) range, up to 2000 nm. Silicon-based alternatives are of interest to replace expensive low band-gap materials, like InGaAs, in telecommunications and imaging applications. Herein, we report on the significant enhancement in NIR photodetector performance afforded by nano- and microstructuring of p-doped silicon (p-Si) prior to deposition of a layer of the organic semiconductor Tyrian Purple (TyP). We show how different silicon structuring techniques, namely, electrochemically grown porous Si, metal-assisted chemical etching, and finally micropylamids produced by anisotropic chemical etching (Si  $\mu$ P), are effective in increasing the NIR responsivity of p-Si/TyP heterojunction diodes. In all cases, the structured interfaces were found to give photodiodes with superior characteristics as compared with planar interface devices, providing up to 100-fold improvement in short-circuit photocurrent, corresponding with responsivity values of 1–5 mA/W in the range of 1.3–1.6  $\mu$ m. Our measurements show this increased performance is neither correlated to optical effects, i.e., light trapping, nor simply to geometric surface area increase by micro- and nanostructuring. We conclude that the performance enhancement afforded by the structured p-Si/organic diodes is caused by a yet unresolved mechanism, possibly related to electric field enhancement near the sharp tips of the structured substrate. The observed responsivity of these devices places them closer to parity with other, well-established, Si-based NIR detection technologies. © 2015 Author(s). All article content, except where otherwise noted, is licensed under a Creative Commons Attribution 3.0 Unported License. [<http://dx.doi.org/10.1063/1.4929841>]

Infrared photodetectors are a major component of many optoelectronic devices used in telecommunications, sensing, and imaging technologies.<sup>1,2</sup> Long distance telecommunications are enabled by silica optical fibers, where near-infrared (NIR) wavelengths in the range of 1.3–1.6  $\mu$ m are used due to the superior transparency of silica in this range. NIR photodetectors are typically fabricated using low-band gap semiconductors, where InGaAs is dominant in most applications.<sup>1–3</sup> Though currently the industry standard due to excellent performance in terms of responsivity and bandwidth, GaAs based technologies are expensive and problematic due to toxicity of precursor materials and difficulties in integration with silicon-based microelectronics. Silicon-based NIR detector solutions would be a highly attractive alternative to incumbent InGaAs technologies.<sup>4</sup> Various methods of sensitizing silicon to function in NIR optoelectronics have been explored in the past. Most early work had focused on doping Si in order to introduce states capable of mid-band gap absorption (MBA).<sup>5</sup> The trade-off between increased responsivity with doping and accompanying decline in

electrical performance is a major obstacle for MBA devices. An alternative concept relies on internal photoemission of electrons from a metallic electrode over a Schottky barrier and into the conduction band of Si.<sup>6,7</sup> These devices are promising; however, their low quantum efficiency has precluded application in telecommunications.<sup>3</sup> “Black silicon” technologies which combine concepts of MBA with nanostructured surfaces to increase absorption have achieved responsivity close to competitive levels for telecom applications.<sup>5,8,9</sup> However, such approaches are still plagued by low charge carrier mobility and overall poor electrical characteristics. In principle, a sensitization approach that does not adversely affect the superior electrical properties of Si is favorable. Silicon/organic heterojunction photodiodes are both low-cost and ecological in comparison with the InGaAs technology, and compatible with silicon-based CMOS. Interest in organic/inorganic heterojunction devices began in the 1980s, and since then several models have been developed to understand the electrical characteristics of such junctions.<sup>9–11</sup> In 2010, it was reported that a heterojunction of a solution-processed fullerene (C<sub>60</sub>) derivative and p-Si displayed a photovoltaic effect down to photon energies of around 0.55 eV (2.25  $\mu$ m),<sup>12</sup> with mediocre NIR responsivity

<sup>a)</sup> Authors to whom correspondence should be addressed. Electronic addresses: eric\_daniel.glowacki@jku.at and ivanda@irb.hr.

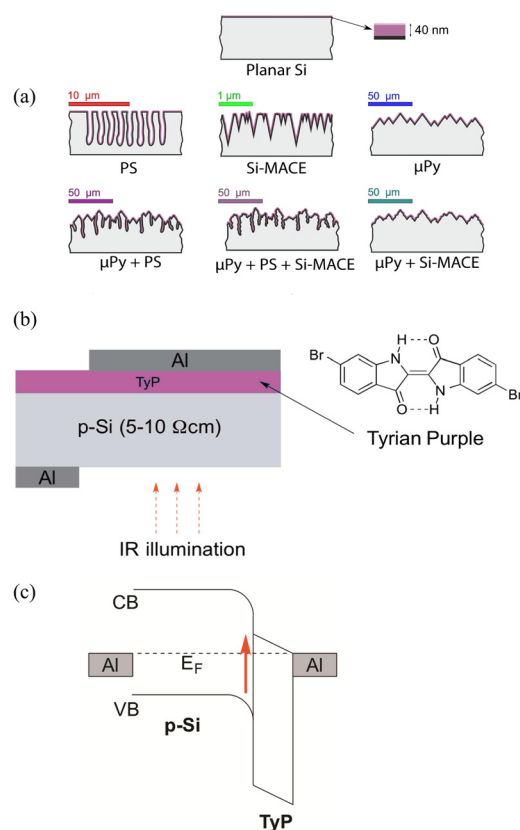


FIG. 1. (a) Schematic representations of structured versus planar heterojunctions between silicon and a thin organic semiconductor epilayer. The upper row shows single-step structuring, while hierarchical combinations of different structuring techniques are on the second row. (b) Device schematic of an Al/p-Si/TyP/Al heterojunction device, with the molecular structure of TyP. (c) Band diagram of an Al/p-Si/TyP/Al heterojunction diode under short circuit conditions, based on findings and assumptions laid out in Refs. 13 and 15. The red arrow represents the sub-band gap NIR absorption.

( $10^{-7}$ – $10^{-5}$  A/W). It only worked at low temperatures (77 K). Improved devices featuring a 20–30 nm-thick vacuum-evaporated organic layer on p-Si, followed this work.<sup>13</sup> With these improvements, and the exchange of C<sub>60</sub> for other organic small

molecules such as indigo and perylene derivatives, the devices gave NIR responsivity around  $1 \times 10^{-4}$  A/W while operating at room temperature and were sensitive down to 2500 nm (0.49 eV). The diodes evaluated here are heterojunction devices between p-Si with micro- and nano-structured surface, and an organic semiconductor Tyrian Purple (6,6'-dibromoin-digo)<sup>14,15</sup> (Figure 1(a)), operated at room temperature. The premise of our work was that micro- and nano-structuring the detector surface would increase the photodetector responsivity due to the increased surface area and light-trapping effects.

Heterojunction diodes with the general device structure as shown in Figure 1(b) were prepared with various nano- and microstructuring methods<sup>16</sup> as shown in Figure 1(a), with planar devices always being prepared in parallel to provide an “internal” standard for a given set of measurements. We have employed a number of well-established techniques to increase the interfacial area of the p-Si/organic junction, both alone and in hierarchical combinations: (1) micropylramids ( $\mu$ -pyramids) with dimensions  $\sim 10$  μm; (2) metal-assisted chemically etched (MACE) porous silicon with  $\sim 50$ – $200$  nm pores; and (3) electrochemically anodized porous silicon, with pore sizes of 10–1000 nm. The structuring methods are explained in detail in the supplementary material.<sup>16</sup> Various silicon structuring methods employed here give feature sizes spanning the range of tens of nanometers up to tens of microns; however, they all exhibit a variety of sharp edges and pointed features. Using the hot-wall epitaxy technique<sup>17</sup> for the deposition of TyP, it was possible to obtain conformal coatings with thickness of 20–40 nm. The growth of these thin films can best be described as Stranski-Krastanov type, with a conformal wetting layer forming with a thickness of  $\sim 10$  nm, followed by growth of TyP crystallites with sizes of tens of nanometers. In Figures 2(a) and 2(b), SEM images of such films on planar p-Si are shown, while Figures 2(c) and 2(d) show the same type of TyP film growth on Si  $\mu$ -pyramids. SEM of porous Si (PSi), and Si MACE, as well as hierarchical combinations of various structuring techniques demonstrates that a remarkably conformal coverage of TyP is achieved on all the structured

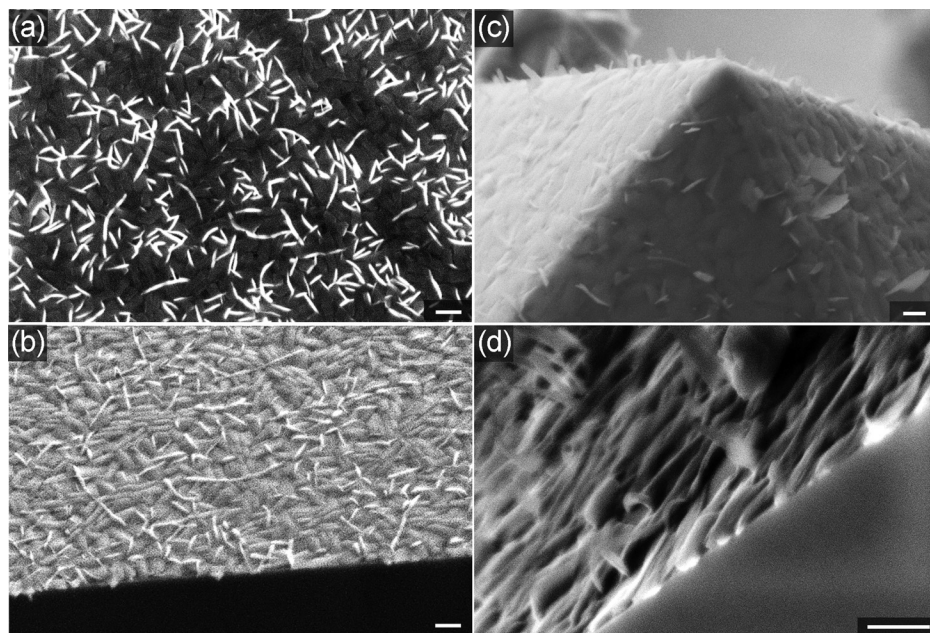


FIG. 2. SEM images of 30–40 nm TyP films grown on planar p-Si (scale bar 200 nm): (a) Top-view, (b) side view of cleaved sample; and on  $\mu$ -pyramid samples: (c) 30° tilted view, (d) side view of cleaved  $\mu$ -pyramid sample. In all cases, the formation of a compact wetting layer is apparent, followed by the growth of TyP crystallites protruding from the surface of the film.



surfaces (Figure 3). Even in the case of very small features (tens of nm range), such as the conical pores on Si MACE (Figures 3(b) and 3(e)), TyP appears to diffuse into these structures and forms a crystalline thin film. Such conformal coverage of organic semiconductor thin films over a wide range of differently structured substrates is not typical, and, in general, deposition conditions need to be finely tuned for each substrate type in order to avoid the less favorable Volmer–Weber type island growth of thin films.<sup>18,19</sup> The hot-wall epitaxy technique we utilized was reported previously to give conformal Stranski-Krastanov films for a perylene bisimide derivative on flat Si substrates.<sup>13</sup> Relatively uniform and continuous coverage of the p-Si with TyP is critical in achieving optimal heterojunction diodes due to the passivation of surface states present at structured silicon surface, in order to avoid the carrier recombination and obtain low dark currents in reverse bias.

Current density-Voltage (J-V) characteristics of the prepared photodiodes were measured in the dark and under illumination with a laser diode emitting at  $1.48\ \mu\text{m}$  with an intensity of  $200\ \text{mW}/\text{cm}^2$ . J-V measurements for dark and

illuminated planar vs. structured samples are shown in Figures 4(a)–4(c), while planar samples compared with hierarchically structured samples are presented in the supplementary material Figure S1.<sup>16</sup> Diodes with a planar interface had a rectification ratio of  $\sim 10^3$ , and under illumination with the laser diode demonstrated a photovoltaic effect with  $J_{\text{SC}} = 1\text{--}5\ \mu\text{A}/\text{cm}^2$  and  $V_{\text{OC}} = 20\text{--}50\ \text{mV}$ . All nano- and microstructuring procedures have led to significant increase in photocurrent, with values of  $J_{\text{SC}}$  between 20 and  $500\ \mu\text{A}/\text{cm}^2$  at short circuit and  $V_{\text{OC}}$  values 10–30 mV higher than planar control samples. At  $-1\ \text{V}$  bias, maximum photocurrents around  $1\ \text{mA}/\text{cm}^2$  could be achieved. Structured interfaces typically showed lower rectification ratio due to higher currents under reverse bias ( $10^2\text{--}10^3$ ). Table I compares the average steady-state photocurrent enhancement, measured at short circuit, over planar samples recorded for the differently structured interfaces under short circuit conditions. Overall,  $\mu$ -pyramids and hierarchical combinations of  $\mu$ -pyramids with PSi and MACE silicon gave the best results, showing 10- to 100-fold improvement in photocurrent over the planar control samples, with the best performing diodes giving a

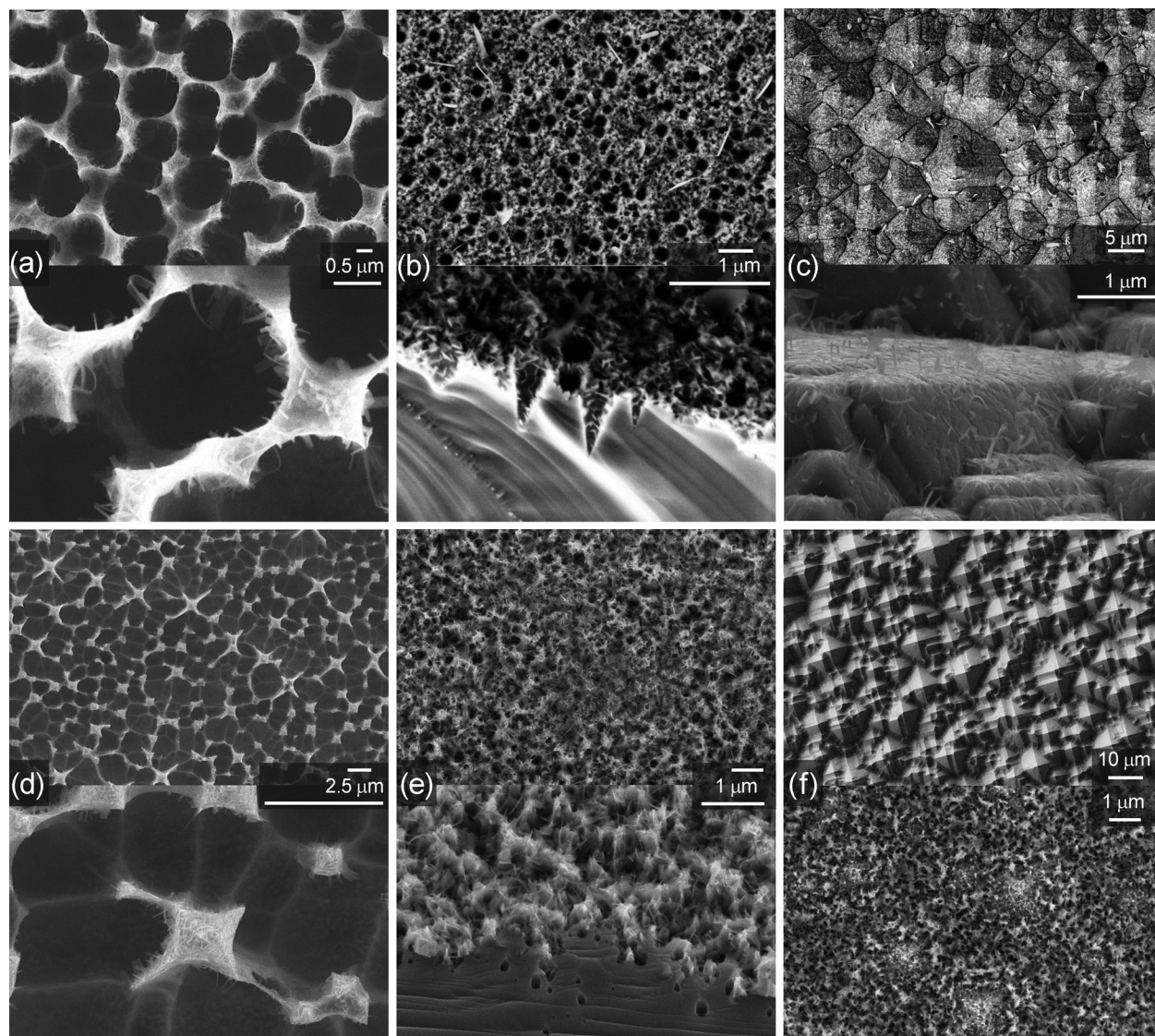


FIG. 3. SEM images of different nano- and microstructured Si surfaces with a 40-nm TyP epilayer evaporated on top. (a) Porous Si, (b) Si MACE, (c) Si  $\mu$ -Pyramids, (d) hierarchical Si  $\mu$ -pyramids/porous Si, (e) hierarchical Si  $\mu$ -pyramids/MACE, and (f) hierarchical Si  $\mu$ -pyramids/MACE/porous Si.

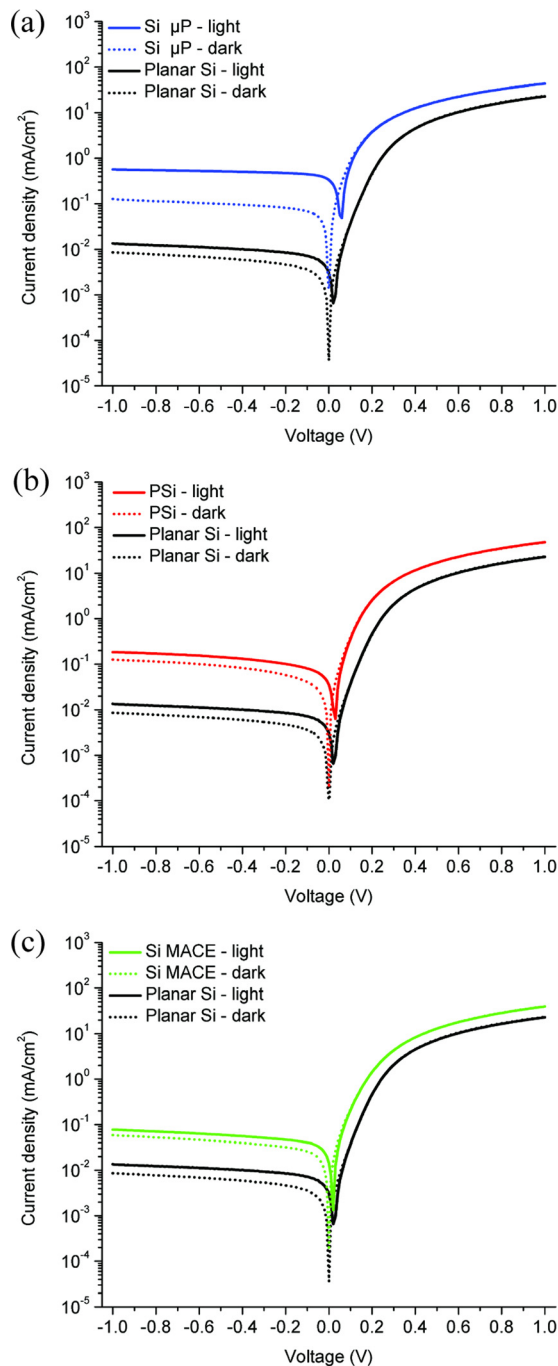


FIG. 4. J-V characteristics of Al/p-Si/TyP/Al in dark and under illumination with a 1.48  $\mu\text{m}$  laser diode ( $200 \text{ mW}/\text{cm}^2$ ). Dark J-V curves are shown with dotted lines, while solid lines represent J-V characteristics under illumination. (a) Comparison of  $\mu$ -pyramid Si with planar devices; (b) Porous Si diodes versus planar; and (c) Si MACE versus planar.

responsivity of 1–5 mA/W in the telecommunication-relevant range of 1.3–1.6  $\mu\text{m}$ . The spectral responsivity is shown in comparison with InGaAs and black silicon devices in supplementary material Figure S2.<sup>16</sup> This difference in performance is probably partly due to the different quality of TyP coverage of the structured silicon surface, as is visible from the J-V curves. The highest  $V_{OC}$  and  $J_{SC}$  are given by the  $\mu$ -pyramid surface, which due to flatness of the  $\mu$ -pyramid sides has the best TyP layer coverage, as is seen in the SEMs in Figures 2 and 3. At the other structures, features such as the bottoms of the pores of PSi and MACE silicon probably have some

TABLE I. Comparison of steady-state short-circuit photocurrent densities generated by nano- and microstructured p-Si/TyP diodes versus the planar control diodes. Values of photocurrent increase factors are given as means and standard deviations over at least six samples for each structuring method.

Structuring method	$J_{sc}/J_{sc\_planar}$
Si $\mu$ -pyramids	$100 \pm 10$
Si $\mu$ -pyramids/Si MACE	$16 \pm 3$
Porous Si/Si $\mu$ -pyramids	$11 \pm 2$
Porous Si	$11 \pm 3$
Si $\mu$ -pyramids/porous Si/Si MACE	$5.0 \pm 0.8$
Si MACE	$4.5 \pm 0.6$

surface exposed and not passivated by the TyP layer, which introduces states responsible for surface recombination and lowering of the  $V_{OC}$  and overall device performance. The etching processes used for structuring are known to increase the amount of surface traps, with the expected trap density scaling as MACE Si > PSi >  $\mu$ -pyramid Si. This expectation is reflected with the observation of  $V_{OC}$  increasing MACE Si < PSi <  $\mu$ -pyramid Si. The role of these charge traps in affording mid-gap absorption is excluded by this finding, as the  $\mu$ -pyramids have the least traps (as concluded from  $V_{OC}$ ) but the highest photocurrent/responsivity.

In order to interpret the origin of the enhancement of photocurrent generation in structured versus planar interfaces, transmission and reflectance of the samples were recorded using an integrating sphere.<sup>20</sup> Figure 5 shows the absorbance of the samples, both with and without the TyP epilayer, while transmission and reflectance are shown in the supplementary material Figure S3.<sup>16</sup> The structured samples have significant absorbance differences in the visible range, at photon energies greater than the band gap of Si. However, in the NIR range (2–1.2  $\mu\text{m}$ ), absorbance of the TyP-covered structured samples is 1%–5% lower than in TyP-planar samples, contrary to what would be expected for observed large  $J_{SC}$  enhancements. Thus, a trivial interpretation of photocurrent increase based on enhanced light absorption by light trapping must be excluded to account for the manifold increase in photocurrent observed in structured

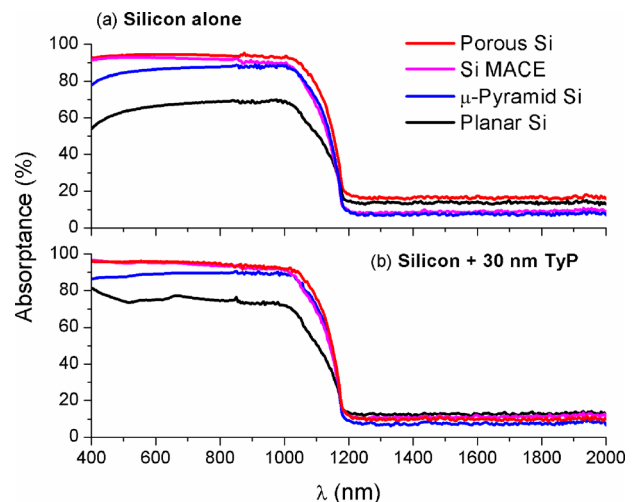


FIG. 5. (a) Absorbance of planar Si, porous Si, Si  $\mu$ -pyramids, and Si MACE; (b) absorbance of the same Si structures with a 40 nm TyP epilayer.



versus planar samples. Further, it would be straightforward to expect the photocurrent enhancement to originate from increased interfacial area between p-Si and TyP, as this correlates directly with the two models for the NIR-absorption mechanism in these diodes, set forth in the literature: (1) a type-II heterojunction transition between the p-Si valance band and organic epilayer conduction band,<sup>12</sup> and (2) absorption by a surface state originating from reactivity of the Si surface and the organic molecular layer.<sup>13,15</sup> However, consideration of the increase in interfacial area also appears insufficient to account for the observed enhancement of photocurrent. For the  $\mu$ -pyramid samples which show the highest  $J_{SC}$  enhancement, for example, the area increases by a factor of 1.55 (calculation based on 3D modeled surface as shown in supplementary material Fig. S4).<sup>16</sup> However, an average 100-fold increase in photocurrent is found. Calculation of the interfacial area produced by the other techniques is not as straightforward as for the  $\mu$ -Pyramids; however, in all cases enhancement in photocurrent is observed. An important finding in this work is that the structuring techniques we have used produce feature sizes from the nm range to the range of tens of  $\mu\text{m}$ , and all have led to substantial responsivity enhancement over planar junctions. It is therefore likely that a common mechanism for enhancement, related to geometrical structuring of silicon, exists. Any eventual explanation of the results presented here hinges upon satisfactory understanding the sub-bandgap sensitization mechanism in p-Si/organic junctions in the first place. We speculate that the large photocurrent enhancement may be related to the concentration of electric field that is produced by sharp pointed structures that originate on all the various structured samples. This hypothesis is consistent with the observation of higher reverse bias current in the case of all structured samples, as enhanced tunneling is expected due to electric field concentration. The increase in photocurrent indeed scales with an accompanying increase in dark current. The increase in photocurrent afforded by the structured interfaces, regardless of the mechanism, represents a significant improvement in performance that brings these devices closer to competitive levels relative to incumbent NIR-sensing platforms.

Sensitizing silicon for infrared detection technologies is of substantial interest for next-generation optoelectronics; however, no silicon-based device concept has yet displaced InGaAs, at least not in telecommunications applications. Herein, we have demonstrated that nano- and microstructured p-Si heterojunctions with an organic semiconductor material may be a promising device concept for Si-based NIR detection. The use of a natural pigment, Tyrian Purple, makes this an inherently greener device, as well as potentially low-cost. Device fabrication involves standard physical vapor deposition and wet-etching techniques, indicating compatibility with CMOS microelectronics. Critical findings include that several different structurization techniques, providing structures spanning the range from 10 nm to 20  $\mu\text{m}$ , all lead to substantial improvement in photocurrent generation over planar interface samples. Responsivity values in the telecom-relevant range, 1.3–1.6  $\mu\text{m}$ , obtained with the

best structured devices are between 1 and 2 mA/W at 0 V bias, increasing to around 5 mA/W at  $-1$  V. These values are a 10-fold improvement over the previous best report of a p-Si/organic NIR diode,<sup>13</sup> while preserving favorable diode characteristics. The mechanism of sensitization that is responsible for the NIR performance of p-Si/organic junctions remains elusive, which makes the interpretation of the substantial improvement given by the structured interfaces problematic. Further research should focus on unraveling this mechanism.

We acknowledge P. Lazić and M. Scharber for valuable discussions. We are grateful for the support by the Austrian Science Foundation, FWF, within the Wittgenstein Prize of N. S. Sariciftci Solare Energie Umwandlung Z222-N19 and the Translational Research Project TRP 294-N19 “Indigo: From ancient dye to modern high-performance organic electronics circuits.” This work has been partly supported by Croatian Science Foundation under the Project No. IP-2014-09-7046. V. Derek was grateful for the support from the Ernst-Mach-Stipendien granted by the OeAD—Austrian Agency for International Cooperation in Education & Research, financed by BMWF, and for financial support by the European Cooperation in Science and Technology through COST Action MP1302 Nanospectroscopy.

<sup>1</sup>R. P. Khare, *Fiber Optics and Optoelectronics*, 1st ed. (Oxford University Press, Oxford, UK, 2004).

<sup>2</sup>*Optoelectronics, Infrared-Visible-Ultraviolet Devices and Applications*, 2nd ed., edited by D. Birtalan and W. Nunley (CRC Press, Boca Raton, Florida, 2009).

<sup>3</sup>A. Rogalski, *Infrared Detectors*, 2nd ed. (CRC Press, Boca Raton, Florida, 2011).

<sup>4</sup>G. Masini, L. Colace, and G. Assanto, *Mater. Sci. Eng.*, **B 89**, 2 (2002).

<sup>5</sup>M. Casalino, *Int. J. Opt. Appl.*, **2**, 1 (2012).

<sup>6</sup>M. K. Lee, C. H. Chu, Y. H. Wang, and S. M. Sze, *Opt. Lett.*, **26**, 160 (2001).

<sup>7</sup>I. Goykhman, B. Desiatov, J. Khurgin, J. Shappir, and U. Levy, *Nano Lett.*, **11**, 2219 (2011).

<sup>8</sup>X. Liu, P. R. Coxon, M. Peters, B. Hoex, J. Cole, and D. Fray, *Energy Environ. Sci.*, **7**, 3223 (2014).

<sup>9</sup>S. R. Forrest, M. L. Kaplan, P. H. Schmidt, and J. M. Parsey, *J. Appl. Phys.*, **58**, 867 (1985).

<sup>10</sup>S. Antohe and A. Vonsovici, *Phys. Status Solidi*, **124**, 583 (1991).

<sup>11</sup>C. K. Renshaw and S. R. Forrest, *Phys. Rev. B*, **90**, 045302 (2014).

<sup>12</sup>G. J. Matt, T. Fromherz, M. Bednorz, S. Zamiri, G. Goncalves, C. Lungenschmied, D. Meissner, H. Sitter, N. S. Sariciftci, C. J. Brabec, and G. Bauer, *Adv. Mater.*, **22**, 647 (2010).

<sup>13</sup>M. Bednorz, G. J. Matt, E. D. Glowacki, T. Fromherz, C. J. Brabec, M. C. Scharber, H. Sitter, and N. S. Sariciftci, *Org. Electron.*, **14**, 1344 (2013).

<sup>14</sup>E. D. Glowacki, L. Leonat, G. Voss, M.-A. Bodea, Z. Bozkurt, A. M. Ramil, M. Irimia-Vladu, S. Bauer, and N. S. Sariciftci, *AIP Adv.*, **1**, 042132 (2011).

<sup>15</sup>M. Bednorz, “Infrared photodetectors based on silicon—Organic hybrid heterojunctions,” Ph.D. dissertation (Johannes Kepler University, 2013).

<sup>16</sup>See supplementary material at <http://dx.doi.org/10.1063/1.4929841> for detailed experimental methods for the nano- and microstructured silicon samples, as well as additional J-V and optical measurements.

<sup>17</sup>H. Sitter, A. Andreev, G. Matt, and N. S. Sariciftci, *Synth. Met.*, **138**, 9 (2003).

<sup>18</sup>S. R. Forrest, *Chem. Rev.*, **97**, 1793 (1997).

<sup>19</sup>W. H. Lee, J. H. Cho, and K. Cho, *J. Mater. Chem.*, **20**, 2549 (2010).

<sup>20</sup>*Handbook of Optics, Volume II - Devices, Measurements, and Properties*, 2nd ed., edited by M. Bass, E. W. Van Stryland, D. R. Williams, and W. L. Wolfe (McGraw-Hill, New York, 1995).